Discover Oncology

Research

Comparative transcriptomic analysis of primary endometrial cancer and bone metastatic cancer: metastasis-associated genes and abnormal cell cycle regulation

Qinmin Wu[1,2,3] · Feng Li[2,3] · Yunlong Zhang[2,3,4] · Siying Li[2,3] · Chuan Xiang[1]

Received: 21 May 2024 / Accepted: 24 January 2025
Published online: 01 February 2025

Abstract

Endometrial cancer (EC) is the most common tumor of the female reproductive system. Its incidence is rising worldwide. Bone metastasis (BMs) in EC is rarely reported, and is seen in only 0.8% of patients. Once bone metastasis develops, it often indicates a poor prognosis. Current research on the bone metastasis of primary tumors suggests that tumor cells primarily colonize bones through hematogenous metastasis and are stimulated to grow by the bone microenvironment. However, the biological mechanism of bone metastasis in EC remains unclear. In this study, we aim to determine the changes in gene expression profiles in EC bone metastasis and explore the transcriptomic differences between metastatic and primary lesions. We collected one primary EC case and two bone metastasis tumors for transcriptomic analysis. The analysis revealed that numerous genes are involved in regulating the cell cycle and proliferation. Analysis of differentially expressed genes (DEGs) revealed that these genes are involved in the regulation of post-translational modification, protein turnover, and signal transduction mechanisms. E2F1, MCM2, RFC2, and ICAM1 are involved in the metastasis and progression of EC with bone metastasis (ECBM). The Kyoto Encyclopedia of Genes and Genomes (KEGG) pathway enrichment analysis indicates significant changes in the Hippo signaling pathway, which regulates cell proliferation, and in the cell adhesion signaling pathway. Numerous transcription factors, including SOX2, NUSAP1, and ACTA1, which promote tumor development, are involved in regulating the expression of cell cycle control genes. Survival curve analysis of high-expression cell cycle genes, including P27, P19, and CDK1, in ECBM showed that elevated levels of these genes are associated with poorer patient survival. Our research identified genes and key signaling pathways associated with bone metastasis. These findings provide a theoretical basis for the treatment of bone metastasis in EC.

Keywords Endometrial cancer · Bone metastatic · Transcriptome characteristics · Cell cycle

Qinmin Wu—First author.

Supplementary Information The online version contains supplementary material available at https://doi.org/10.1007/s12672-025-01850-7.

✉ Chuan Xiang, chuanxiang@sxmu.edu.cn; Qinmin Wu, gui625625625@163.com | [1]Department of Orthopedics, Second Hospital of Shanxi Medical University, Taiyuan 030001, Shanxi, China. [2]Weifang People's Hospital, Weifang 261000, Shandong, China. [3]The First Affiliated Hospital of Shandong Second Medical University, Weifang 261000, Shandong, China. [4]Shandong Second Medical University, Weifang 261000, Shandong, China.

1 Background

EC is the fourth cancer among women worldwide, after breast, lung, bronchus and colon, rectum [1]. The incidence of EC is rising worlwilde, and women are still dying from the disease with a 5-year overall survival reaching 80% [2, 3]. EC-related deaths are mostly due to distant metastases reducing overall survival [4]. Although most EC patients are diagnosed at an early stage with a favorable prognosis, approximately 5–30% of all patients with EC experience recurrence or distant metastasis following the initial treatment, with a 5-year survival rate of only 17 percent [5]. There are no standard treatment options for metastatic endometrial cancer and some patients respond poorly to conventional treatment, leading to a poor prognosis [6]. Therefore, understanding the molecular characteristics of bone metastasis in endometrial cancer is very important to improve the prognosis of patients.

Distant metastatic patterns of EC usually include: intra-abdominal metastasis, distant lymph node involvement or distant organ metastasis (lung, liver, brain or bone) [7, 8]. BM rarely occurs in EC compared to other cancers such as breast, lung, renal, and prostate cancer and less studied. The incidence of bone metastasis has been reported to be 39.3% of all distant metastases [9]. EC undergoes bone metastasis through the bloodstream, and bone metastases are often more common in the body's axial bones, such as the spine and pelvis [10]. EC with pelvic metastasis is more common than spinal metastasis. Secondly, EC is also prone to metastasis to the ribs, femur, and humerus [11].

In the present study, we performed transcriptome sequencing on non metastatic EC and bone metastatic EC through genetic testing, the metastatic pattern of bone metastases occurring in EC was systematically summarized. The research results can be used for risk assessment of cancer recurrence, selecting appropriate targeted drugs through tissue testing, guiding immunotherapy, and also helpful for traditional chemotherapy. Medical testing at the molecular biology level predicts survival and distant metastasis in EC patients.

2 Materials and Methods

2.1 Human samples

Three tissue specimens were collected from the First Affiliated Hospital of Shandong Second Medical University (Weifang People's Hospital) from April 2023 to September 2023, including one case of EC tissue and two cases of EC spinal metastasis tissue. The samples were confirmed by the immunohistochemical (IHC). Written informed consents were obtained from all participants. Ethical approval for this study was granted by the ethics committee of Weifang People's Hospital.

2.2 RNA extraction

RNA was extracted using the RNeasy Mini Kit from QIAGEN, following the provided instructions. All reagents and consumables used in the experiment were RNase-free. The specific steps were as follows: 1. Cell Lysis: 350 µl of Buffer RLT, containing 1% β-mercaptoethanol, was added to the cells, and the mixture was thoroughly pipetted to resuspend the cells. 2. Ethanol Addition: 350 µl of 70% absolute ethanol was added, mixed by pipetting, and the solution was transferred to the adsorption column. The mixture was then centrifuged at 10,000 g for 15 s, and the effluent was discarded. 3. Wash with Buffer RW1: 350 µl of Buffer RW1 was added, and the mixture was centrifuged at 10,000 g for 15 s. The effluent was discarded. 4. DNase Treatment: 10 µl of DNaseI was mixed with 70 µl of Buffer RDD, and the solution was added vertically to the membrane of the adsorption column, ensuring full contact with the membrane. The column was left at room temperature for 15 min. 5. Second Wash with Buffer RW1: 350 µl of Buffer RW1 was added, and the column was centrifuged at 10,000 g for 20 s. 6. Third Wash with Buffer RW1: 350 µl of Buffer RW1 was added, and the column was centrifuged at 10,000 g for 20 s. 7. Wash with Buffer RPE: 500 µl of Buffer RPE was added, and the column was centrifuged at 10,000 g for 2 min. The flow-through was discarded. 8. Final Spin: The collection tube was replaced, and the column was centrifuged at maximum speed for 2 min. 9. RNA Elution: The adsorption column was placed in a 1.5 ml centrifuge tube, and approximately 30 µl of RNase-free water was added based on the amount of cells. The column was left to stand for 1 min, and then centrifuged at 8000 rpm for 1 min to collect the RNA.

2.3 Reverse transcription of RNA to cDNA

The M-MLV Reverse Transcriptase system from Invitrogen was used according to the product instructions. a. The following components were mixed in a 200 µl PCR tube: oligo (dT) (500 µg/ml) 1 µl, dNTP (10 mM) 1 µl, total RNA 2 µg, and RNase-free water up to 12 µl. b. The mixture was heated and denatured in a PCR instrument at 65℃ for 5 min, then quickly cooled on ice. c. The following components were then mixed in the PCR tube: 5 × First-strand buffer 4 µl, DTT (0.1 M) 2 µl, RNase Inhibitor (20 U/µl) 1 µl, and M-MLV 1 µl. d. The ingredients from step c were combined and 8 µl of the mixture was added to each PCR tube from step b. The reaction was performed in the PCR instrument at 37℃ for 60 min, followed by 70℃ for 15 min to inactivate M-MLV.

2.4 Kaplan–Meier plotter analysis

Kaplan–Meier plotter analysis. The prognostic value of P27, P19, and CDK1 in EC have been analyzed using the Kaplan–Meier Plotter (http://kmplot.com/analy sis/), a database that integrates gene expression data and clinical data. We focused our analysis on overall survival (OS). The hazard ratio with 95% confidence intervals and log rank p value were calculated. We analyzed the best specific probes (JetSet probes) that recognized P27, P19, and CDK1 to reduce our false discovery rate, and selected $p < 0.05$ as the threshold.

2.5 RNA-seq

To ensure the quality of samples used for transcriptome sequencing, advanced molecular biology equipment was employed by Baimaike Biosequencing Inc. The purity, concentration, and integrity of the extracted total RNA were rigorously detected. The total RNA quality detection methods included: (1) The purity and concentration of RNA were detected using a NanoDrop 2000 spectrophotometer. (2) RNA integrity was precisely assessed using Agent2100/LabChip GX detection.

The main process of library construction involves the following steps: (1) Eukaryotic mRNA was enriched using magnetic beads containing Oligo (dT); (2) Fragmentation Buffer was added to randomly disrupt the mRNA; (3) The first and second cDNA strands were synthesized using mRNA as a template, followed by the purification of the cDNA; (4) The purified double-stranded cDNA underwent end repair, an A-tail was added, and sequencing adapters were connected. The fragment size was then selected using AMPure XP beads; (5) Finally, a cDNA library was obtained through PCR enrichment.

Library quality control: Once the library construction is finished, initial quantification is performed using the Qubit 3.0 fluorescence quantitative analyzer, with a required concentration of 1 ng/µl or higher. Subsequently, the library's inserted fragments are identified utilizing the Qsep400 high-throughput analysis system. After ensuring that the inserted fragments meet the criteria, the library's effective concentration (greater than 2 nM) is precisely measured using the Q-PCR method to ensure library quality.

For machine sequencing, the Illumina NovaSeq6000 sequencing platform was employed in PE150 mode after the library passed quality inspection.

Analysis process: Once the sequencing data were retrieved from the machine, bioinformatics tools provided by BMK-Cloud (www.biocloud.net) on the Baimaike cloud platform were utilized for analysis. The offline data were filtered to obtain clean data, sequences were aligned with the specified reference genome, and mapped data were generated. Subsequently, library quality evaluation, structural analysis, differential expression analysis, gene functional annotation, and functional enrichment were conducted. Furthermore, via the BMKCloud platform (www.biocloud.net), comprehensive data mining analysis was conducted to accomplish a variety of personalized interactive transcriptome operations, including gene retrieval mapping, analysis of unique and shared genes, construction of protein interaction networks, gene set enrichment analysis (GSEA), differential gene co-expression analysis, and construction of gene co-expression networks (WGCNA)..

3 Results

3.1 Overall mRNA expression in EC and ECBM

ECBM is classified as an advanced malignant tumor. Squamous cell carcinoma is a common pathological type [12]. The main treatment methods are surgery, radiotherapy, and chemotherapy [13]. It is crucial to select treatment plans

based on the pathological type and extent of metastasis. With the rapid advancement of precision medicine and sequencing technologies, gene expression sequencing provides a theoretical basis for selecting treatment methods. We selected one sample of EC in situ and two samples of ECBM for transcriptome sequencing (Fig. 1A, B). Sample correlation analysis revealed significant outliers in EC in situ samples and in two bone metastasis samples. Gene expression differs significantly between these two sample types. The gene expression patterns in bone metastasis samples from two patients are similar and reproducible, suggesting consistent gene expression patterns in bone metastasis cancer (Fig. 1C). Creating box plots of gene expression levels for each sample allows for visualization of the dispersion within individual samples and facilitates an intuitive comparison of gene expression levels across different samples. The box plot of FPKM distribution in this study indicates minimal variation in gene expression levels and dispersion across the samples. (Fig. 1D). The total number of differentially expressed genes between ECBM and in situ EC is 4,309. Among these, 2,311 genes are upregulated, while 1,998 genes are downregulated. (Fig. 1E). We used volcano plots and heat maps to display genes with significant expression differences. For example, genes such as PCOLCE, SPP1, and KRT8 were significantly upregulated, contributing to tumor formation and development. (Fig. 1F, G).

3.2 Different physiological functions regulated by differentially expressed genes in ECBM compared to EC

The expression of genes is influenced by various factors, including alternative splicing. Precursor mRNA generated by transcription can undergo multiple splicing processes, where different exons are selected to produce distinct mature mRNA molecules. These mRNA variants are then translated into different proteins, contributing to the diversity of biological traits. This process of post-transcriptional mRNA modification is known as alternative splicing. The various types of alternative splicing are illustrated in the accompanying figure (Fig. 2A). We separately observed the types, quantities, and proportions of variable splicing events in EC and ECBM. The results show that a significant number of variable splicing events occur in both EC and ECBM, which is a crucial factor contributing to changes in gene expression levels. (Fig. 2B). Compared to ECBM, EC exhibited significant changes in numerous genes. We classified and statistically analyzed the functions of the differentially expressed genes using COG (Clusters of Orthologous Groups of proteins) (Fig. 2C). The experimental results demonstrate that numerous differentially expressed genes are involved in the regulation of post-translational modification, protein turnover, cell cycle, and signal transduction mechanisms (Fig. 2C). Previous studies have shown that these signaling pathways are involved in the proliferation and migration of tumor cells. We used the Gene Ontology (GO) Consortium to perform functional annotation on differentially expressed genes. The GO annotation system is organized as a directed acyclic graph, consisting of three main branches: biological process, molecular function, and cellular component. Each term in the GO system represents a basic unit (entry or node), and corresponds to a specific attribute. By using the gene annotation results, differentially expressed genes can be classified and statistically analyzed at the secondary classification level of the GO database. This approach allows for a clearer understanding of the primary functional categories associated with these genes [14]. According to the analysis, numerous genes are involved in regulating cellular processes, biological regulation, cellular anatomical structures, intracellular activities, binding, and catalytic activities (Fig. 2D). We observed that many differentially expressed genes are involved in DNA replication and cell cycle regulation. (Fig. 2E). Tumor occurrence and progression are closely linked to the cell cycle and DNA replication processes.

3.3 ECBM shows significant changes in cell cycle related genes compared to EC

Compared to EC, ECBM exhibits significant changes in genes related to the cell cycle. (Fig. 3A). By selecting the top 10 enriched GO terms and creating an enrichment chord diagram, we observed that a significant number of genes are involved in regulating the cell cycle and proliferation. (Fig. 3B, Figure S1-A). For example, key genes such as E2F1, MCM2, RFC2, and ICAM1 are implicated in the metastasis and progression of ECBM. Many highly expressed genes in ECBM are involved in the synthesis of cytosolic components, the actin cytoskeleton, the MCM complex, chromosomes, centromeres, and the endoplasmic reticulum. This suggests that the cells are in a state of rapid proliferation. (Fig. 3C, D, Figure S1-B). The rapid proliferation of cells demands substantial energy. In genes highly expressed in ECBM, a significant number are involved in ATP synthesis. (Fig. 3E, F, Figure S1-C). Both the rapid accumulation of cellular components and the rapid synthesis of ATP prepare the cells for swift proliferation, facilitating an efficient mode of cell growth.

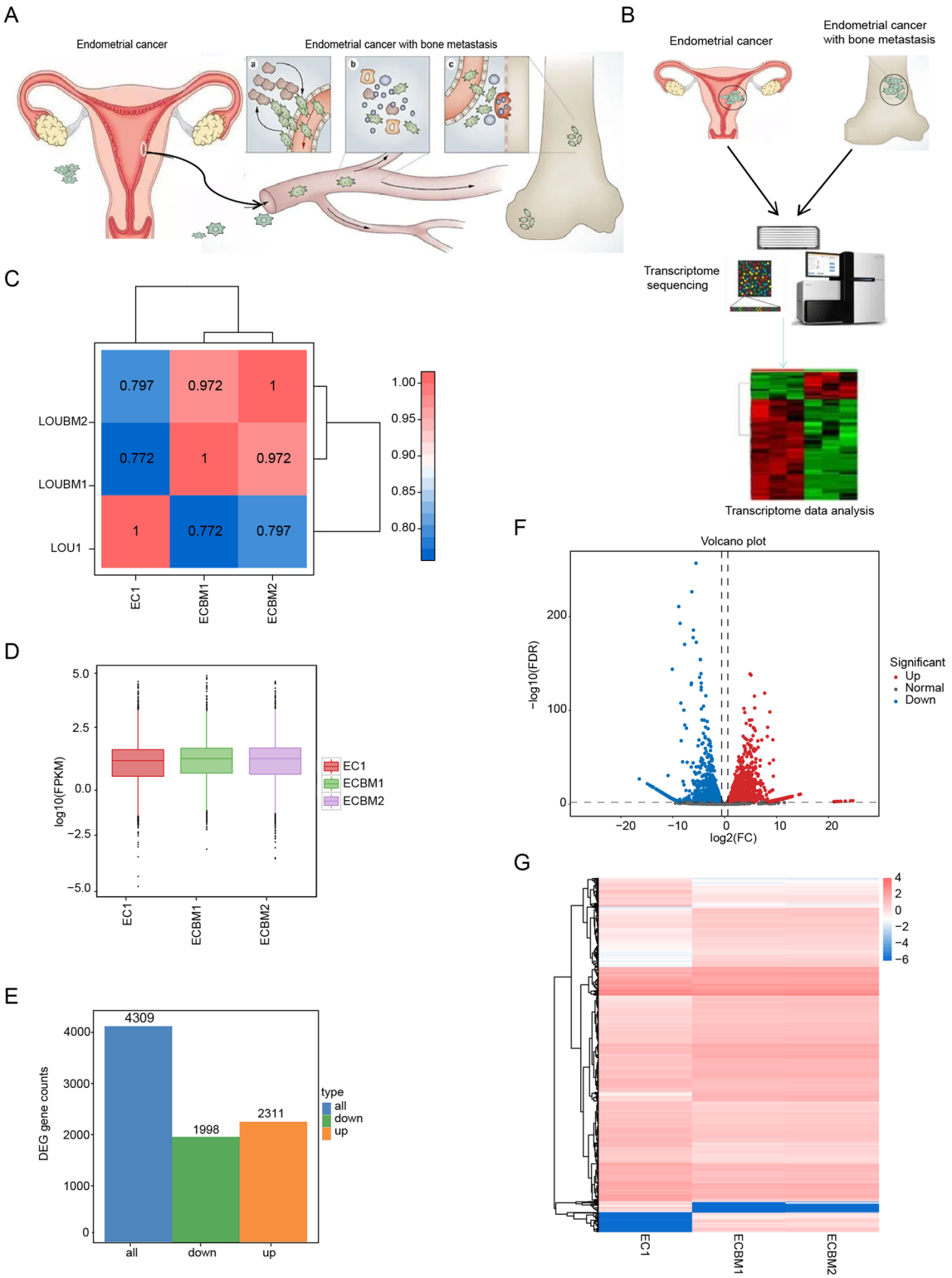

Fig. 1 Gene expression profiling of EC and ECBM tissues. **A** Flow chart of the mechanism of ECBM. **B** The second generation sequencing platform was used to analyze the transcriptome of 3 samples of EC and ECBM tissues. **C** Heat map of expression correlation between EC and ECBM tissues. **D** Boxplots of FPKM for EC and ECBM tissues. **E** Number of genes in differentially expressed gene sets. Blue represents all differentially expressed genes, orange represents up-regulated genes, and green represents down-regulated genes. **F, G** The volcano plot and heat map shows the differentially expressed genes between EC and ECBM tissues

Fig. 2 Different physiological functions regulated by differentially expressed genes in ECBM compared to EC. **A** (A) Exon jumping and multi ▶ exon jumping; **B** Single intron preservation and multi intron preservation; **C** Variable exons; **D** Variable transcription start site; **E** Variable transcription termination site; The red area represents the variable splicing type.**B.** The horizontal axis represents variable cut events, while a vertical axis represents variable cut classes. (1) TSS: Alternative 5 'first exon (transcription start site); (2) TTS: Alternative 3 'last exon (transcription terminal site); (3) SKIP: Skipped exon (SKIP_ON, SKIP_OFF pair); (4) XSKIP: Approximate SKIP (XSKIP_ON, XSKIP_OFF pair) single exon skipping (blurred boundaries); (5) MSKIP: Multi exon SKIP (MSKIP_ON, MSKIP_OFF pair); (6) XMSKIP: Proximate MSKIP (XMSKIP_ON, XMSKIP_OFF pair) multiple exon jumps (blurred boundaries); (7) IR: Intron retention (IR-ON, IR-OFF pair); (8) XIR: Proximate IR (XIR-ON, XIR-OFF pair) single intron retention (blurred boundary); (9) MIR: Multi IR (MIR-ON, MIR-OFF pair) multiple intron retention; (10) XMIR: Proximate MIR (XMIR-ON, XMIR-OFF pair) with multiple intron retention (blurred boundaries); (11) AE: Alternative exit ends (5 ', 3', or both); (12) XAE: Approximate AE variable 5 'or 3' end shear (blurred boundary). **C** Classification of differentially expressed genes by COG annotation. **D** GO enrichment bubble plot of differentially expressed genes. **E** GO annotation system for differentially expressed genes. The abscissa is the GO classification, the ordinate is the number of genes, blue is the Biological Process, green is the Cellular Component, and yellow is the Molecular Function

3.4 Functional enrichment analysis of differentially expressed genes in EC and ECBM

Different gene products coordinate to perform various biological functions. Annotating pathways for differentially expressed genes can provide deeper insights into gene functions. The KEGG (Kyoto Encyclopedia of Genes and Genomes) database systematically analyzes gene functions and genomic information. Researchers can use KEGG to study genes and their expression comprehensively. As the primary public pathway database (Kanehisa, 2008), KEGG offers integrated metabolic pathway searches. The database includes processes such as the biodegradation of organic matter, carbohydrate metabolism, nucleoside metabolism, and amino acid metabolism. We compared the differential genes and metabolic pathways between ECMB and EC, providing comprehensive annotations for the enzymes involved in each reaction step. This includes amino acid sequences and links to PDB entries. The KEGG annotation results for differentially expressed genes were categorized according to KEGG pathway types, offering valuable insights for in vivo metabolic analysis and metabolic network research. (Fig. 4A). The KEGG signaling pathway analysis reveals that numerous genes are involved in tumor formation and development. (Fig. 4B). We observed significant changes not only in the cell cycle but also in the Hippo signaling pathway, which regulates cell proliferation. Additionally, the adhesion regulation signaling pathways between cells also showed considerable alterations. These changes may be important factors contributing to tumor metastasis. (Fig. 4C, D). We also analyzed changes in immune-related regulation and identified significant alterations in the immune regulatory signaling pathways associated with ECBM. These alterations include changes in immune response and regulation, which are accompanied by abnormal activation of cellular activities. (Fig. 4E, Figure S2).

3.5 Genes with high expression of ECBM promote malignant characterization of tumors

The transcription factor binding site (TFBS) is a DNA sequence that interacts with transcription factors, usually ranging from 5 to 20 base pairs in length [15]. A transcription factor often regulates multiple genes simultaneously. The binding sites of a transcription factor on different genes exhibit a degree of conservation, though they are not entirely identical [15]. We used the R package TFBS Tools to predict transcription factor binding sites (TFBS) in the promoter regions of differentially expressed genes, defining approximately 1 kb upstream of each gene as a potential promoter region. This analysis was conducted with reference to the JASPAR database for transcription factor motifs (http://jaspar.genereg.net/) [16, 17]. By analyzing the binding sites of transcription factors, we can identify which transcription factors regulate gene expression and gain further insight into the regulatory mechanisms involved. We conducted a transcription factor locus analysis on genes with high expression in ECBM and discovered that numerous transcription factors associated with tumor occurrence and development are involved in the regulation of cell cycle regulatory genes. For example, factors such as SOX2, NUSAP1, and ACTA1 were identified (Fig. 5A). The highly expressed cell cycle genes in ECBM include P27, P19, and CDK1. We analyzed the survival curves associated with these genes (http://www.kmplot.com/) (Fig. 5B). The analysis results indicate that high expression of these genes is associated with decreased patient survival. Additionally, abnormal cell cycle regulation may contribute to the malignant characteristics of ECBM. Fusion genes are chimeric genes formed by connecting the coding regions of two or more genes end-to-end and placing them under the control of the same set of regulatory sequences (including promoters, enhancers, ribosomal binding sequences, and terminators). These fusion genes exhibit novel functions or functions distinct from those of the original genes and are specifically expressed under certain conditions [18]. We utilized Fusionmap to investigate gene fusion events in the transcriptome. Fusionmap initially identifies potential

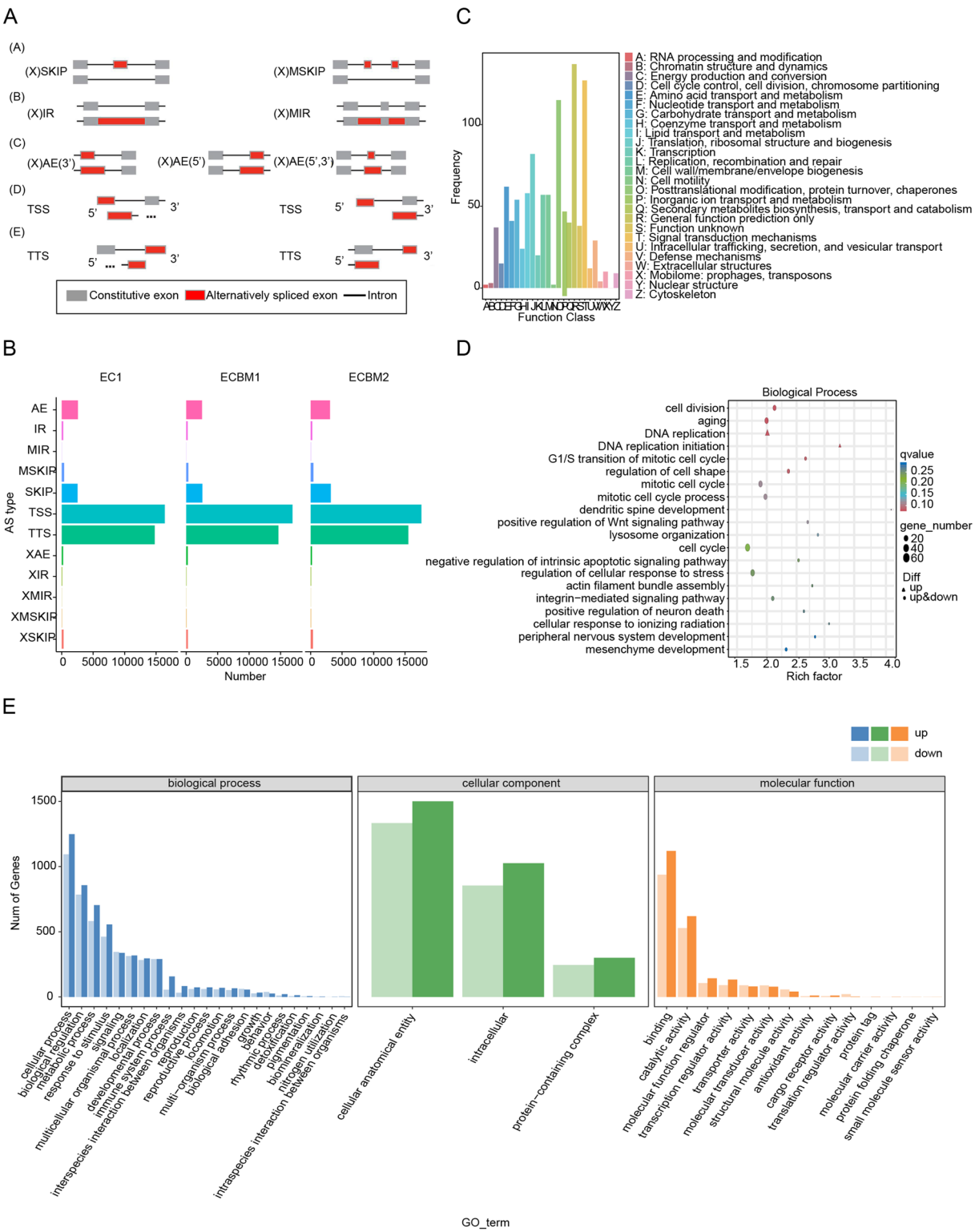

gene fusions by aligning sequences based on paired-end relationships within the genome and transcripts. It then filters out false positives by comparing results with databases such as NT. We observed significant differences in gene fusion rates between EC and ECBM. Specifically, the fusion rate was higher in EC compared to ECBM, which

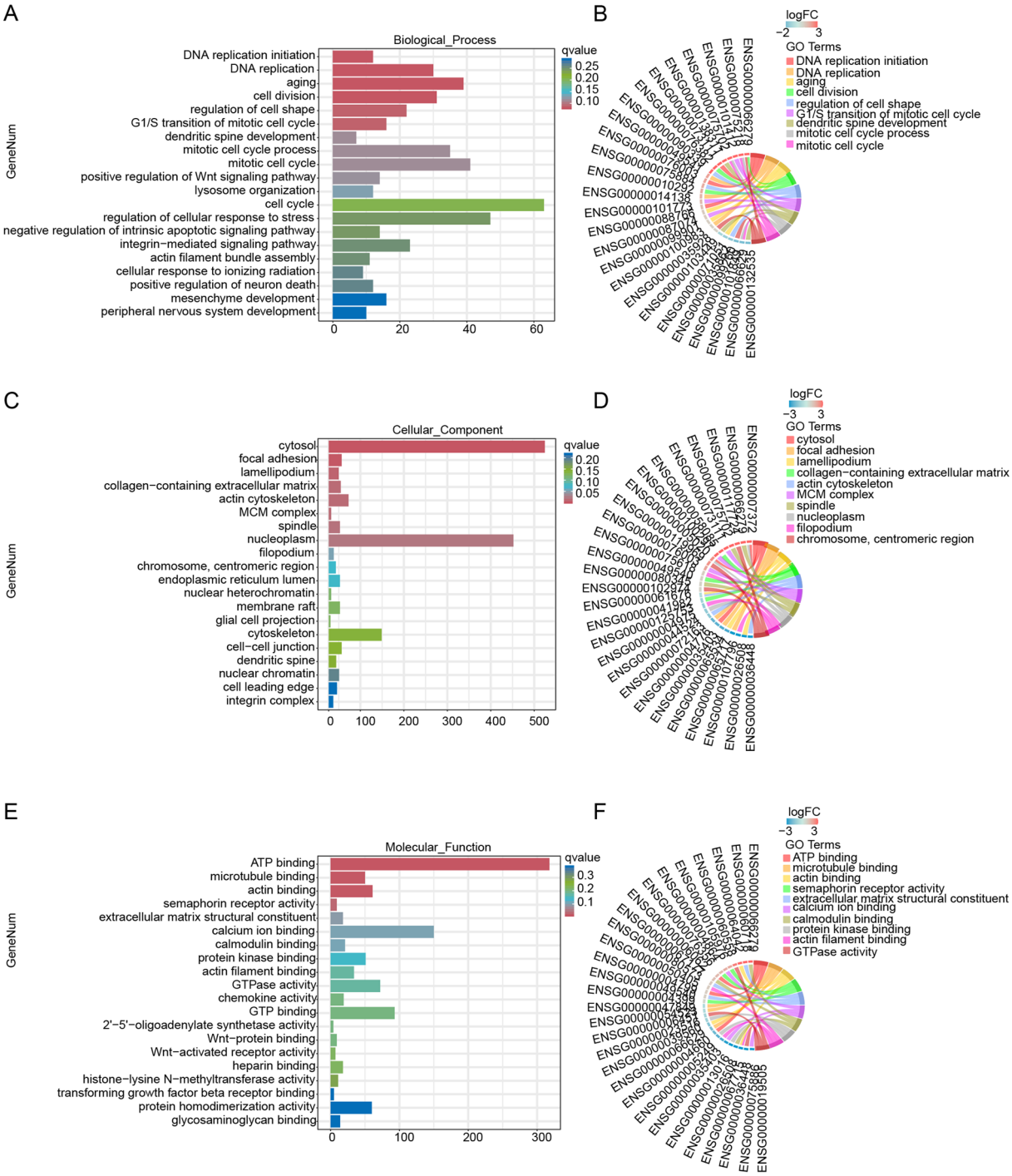

Fig. 3 Changes in cell cycle-related genes in EC compared to ECBM. **A**, **B** The biological processes of GO enrichment of differentially expressed genes were visualized using bar graphs and enriched string plots. **C**, **D** The cellular component enriched by GO of differentially expressed genes were visualized using bar graphs and enriched string plots. **E**, **F** The molecular function enriched by GO of differentially expressed genes were visualized using bar graphs and enriched string plots

exhibited a lower fusion rate. These findings suggest that the occurrence of bone metastasis indeed leads to cellular reprogramming (Fig. 5C). We speculate that the cell cycle in EC cells is longer, which increases the likelihood of gene

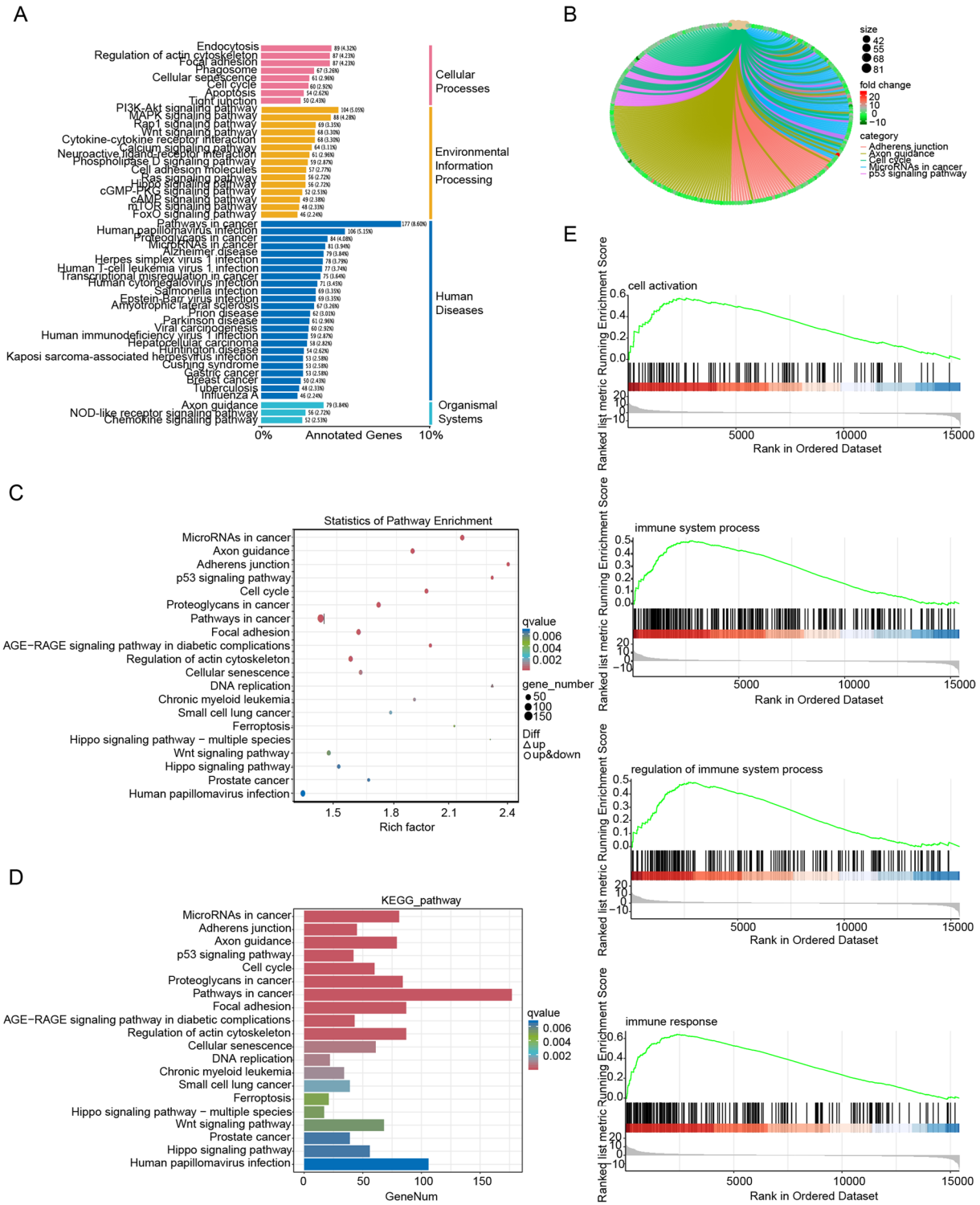

Fig. 4 Functional enrichment analysis of differentially expressed genes in EC and ECBM. **A** KEGG classification map of differentially expressed genes **B** The network diagram was used to visualize the enrichment degree of differentially expressed genes and KEGG pathways. **C**, **D** The KEGG enriched pathways of differentially expressed genes between EC and ECBM were visualized using bubble plots and bar graphs. **E.** GSEA analysis used KEGG pathway and GO as the gene set. The enrichment of cell activation, immune system process, regulation of immune system process and immune response was analyzed

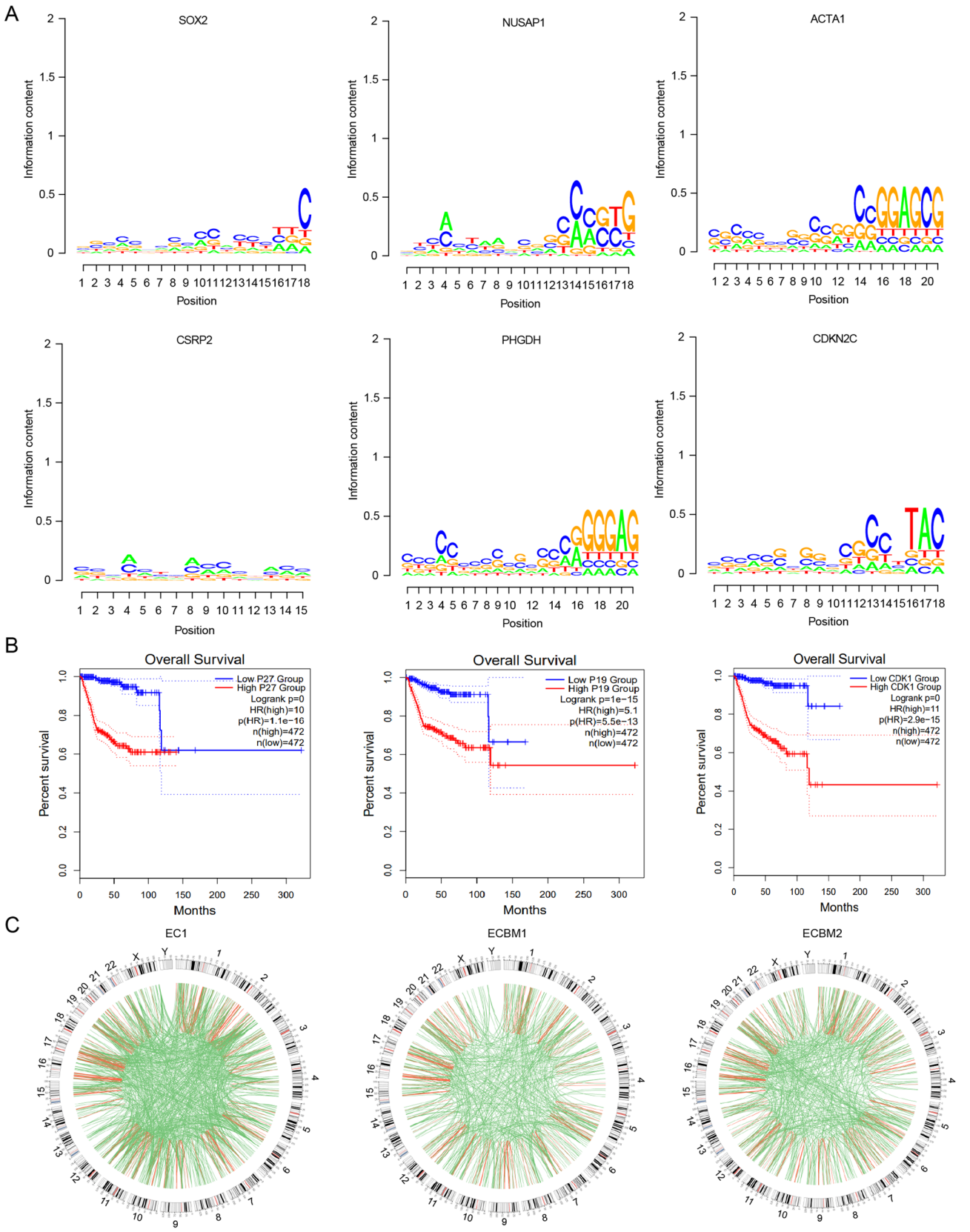

Fig. 5 Genes with high expression of ECBM promote malignant characterization of tumors. **A** Transcription factor binding site motif. **B** Kaplan–Meier survival curves of patients with high and low expression of P27, P19, and CDK1. **C.** The gene fusion events detected were in EC1, ECBM1, and ECBM2

fusion events. In contrast, the cell cycle in ECBM cells is shorter, leading to accelerated proliferation and a decreased probability of gene fusion.

4 Discussion

EC is one of the most common malignancies in the female reproductive system and has a mortality rate that is second only to ovarian and cervical cancers [18–20]. It often leads to distant metastases, with bone metastasis being the most common site [6]. In this study, we collected tissue samples from one non-metastatic EC and two bone metastatic tumors for transcriptome sequencing. We analyzed the biological data to offer insights for future research on EC. The results revealed significant differences in gene expression between the two sample groups. Most differentially expressed genes were associated with the regulation of the cell cycle and proliferation. Additionally, we observed notable alterations in the signaling pathways that control intercellular adhesion. We believe this may play a crucial role in tumor metastasis. According to the Kaplan–Meier mapping database, the increased expression of genes such as P27, P19, and CDK1, which are highly expressed in ECBM, is correlated with poorer prognosis. In conclusion, the significant differences in gene expression between non-metastatic EC and bone metastatic tumor tissues, as well as the occurrence of bone metastasis, suggest that tumor cells undergo reprogramming. These findings provide valuable insights for future in-depth studies on EC.

Acknowledgements We thank Si-Ying Li, a research assistant in our laboratory, for submitting this manuscript to the journal and for continuing to follow up on the status of this manuscript.

Author contributions Q.W. designed and conducted the experiment and wrote the manuscript. F.L. prepared the materials. Y.Z. supported the execution of research. S.L. reviewed and edited the manuscript and assisted in its submission, and C.X. wrote, reviewed, and revised the manuscript. All authors read and approved the final manuscript.

Funding Not funding.

Data availability The datasets generated during and/or analyzed during the current study are available from the corresponding author upon reasonable request.

Declarations

Ethics approval and consent to participate This study was conducted in accordance with the principles of the Declaration of Helsinki. This study was also approved and performed by Weifang People's Hospital. Written informed consent was obtained from the patients for the publication of this article.

Competing Interests The authors declare no competing interests.

References

1. Li H, Xiao Z, Xing B, et al. Association between common vaginal and HPV infections and results of cytology test in the Zhoupu District, Shanghai City, China, from 2014 to 2019. Virol J. 2022;19(1):127. https://doi.org/10.1186/s12985-022-01850-x.
2. Ramchander NC, Ryan NAJ, Walker TDJ, et al. Distinct immunological landscapes characterize inherited and sporadic mismatch repair deficient endometrial cancer. Front Immunol. 2019;10:3023. https://doi.org/10.3389/fimmu.2019.03023.
3. Bosse T, Nout RA, McAlpine JN, et al. Molecular classification of grade 3 endometrioid endometrial cancers identifies distinct prognostic subgroups. Am J Surg Pathol. 2018;42(5):561–8. https://doi.org/10.1097/PAS.0000000000001020.
4. Han J, Zhang L, Guo H, et al. Glucose promotes cell proliferation, glucose uptake and invasion in endometrial cancer cells via AMPK/mTOR/S6 and MAPK signaling. Gynecol Oncol. 2015;138:668–75. https://doi.org/10.1016/j.ygyno.2015.06.036.
5. Urick ME, Bell DW. Clinical actionability of molecular targets in endometrial cancer. Nat Rev Cancer. 2019;19(9):510–21.

6. Nguyen QN, Chun SG, Chow E, et al. Single-fraction stereotactic vs conventional multifraction radiotherapy for pain relief in patients with predominantly nonspine bone metastases: a randomized phase 2 trial. JAMA Oncol. 2019;5(6):872–8. https://doi.org/10.1001/jamaoncol.2019.0192.
7. Uccella S, Morris JM, Multinu F, et al. Primary brain metastases of endometrial cancer: a report of 18 cases and review of the literature. Gynecol Oncol. 2016;142(1):70–5.
8. Mao W, Wei S, Yang H, et al. Clinicopathological study of organ metastasis in endometrial cancer. Future Oncol. 2020;16(10):525–40.
9. Zheng Y, Jiang P, Tu Y, et al. Incidence, risk factors, and a prognostic nomogram for distant metastasis in endometrial cancer: a SEER-based study. Int J Gynaecol Obstet. 2024;165(2):655–65. https://doi.org/10.1002/ijgo.15264.
10. Skrajnowska D, Jagielska A, Ruszczyńska A, et al. Effect of copper and selenium supplementation on the level of elements in rats' femurs under neoplastic conditions. Nutrients. 2022;14:6. https://doi.org/10.3390/nu14061285.
11. Shi R, Zhang W, Zhang J, et al. CircESRP1 enhances metastasis and epithelial-mesenchymal transition in endometrial cancer via the miR-874-3p/CPEB4 axis. J Transl Med. 2022;20(1):139. https://doi.org/10.1186/s12967-022-03334-6.
12. Bi Q, Li Q, Yang J, et al. Preliminary application of magnetization transfer imaging in the study of normal uterus and uterine lesions. Front Oncol. 2022;12: 853815. https://doi.org/10.3389/fonc.2022.853815.
13. Ma AY, Xie SW, Zhou JY, et al. Nomegestrol acetate suppresses human endometrial cancer RL95–2 cells proliferation in vitro and in vivo possibly related to upregulating expression of SUFU and Wnt7a. Int J Mol Sci. 2017;18(7):1. https://doi.org/10.3390/ijms18071337.
14. Zhou S, Chen L, Chen G, et al. Molecular mechanisms through which short-term cold storage improves the nutritional quality and sensory characteristics of postharvest sweet potato tuberous roots: a transcriptomic study. Foods. 2021;10:9. https://doi.org/10.3390/foods10092079.
15. Shen LC, Liu Y, Song J, et al. SAResNet: self-attention residual network for predicting DNA-protein binding. Brief Bioinform. 2021;22:5. https://doi.org/10.1093/bib/bbab101.
16. Tan G, Lenhard B. TFBSTools: an R/bioconductor package for transcription factor binding site analysis. Bioinformatics. 2016;32(10):1555–6. https://doi.org/10.1093/bioinformatics/btw024.
17. Peghaire C, Dufton NP, Lang M, et al. The transcription factor ERG regulates a low shear stress-induced anti-thrombotic pathway in the microvasculature. Nat Commun. 2019;10(1):5014. https://doi.org/10.1038/s41467-019-12897-w.
18. Jia W, Li H, Li S, et al. Oviz-Bio: a web-based platform for interactive cancer genomics data visualization. Nucleic Acids Res. 2020;48(W1):W415–26. https://doi.org/10.1093/nar/gkaa371.
19. Song Y, Huang J, Wang K, et al. To identify adenomatous polyposis coli gene mutation as a predictive marker of endometrial cancer immunotherapy. Front Cell Dev Biol. 2022;10: 935650. https://doi.org/10.3389/fcell.2022.935650.
20. Zong ZH, Liu Y, Chen S, et al. Circ_PUM1 promotes the development of endometrial cancer by targeting the miR-136/NOTCH3 pathway. J Cell Mol Med. 2020;24(7):4127–35. https://doi.org/10.1111/jcmm.15069.